Chlorophyll-a fluorescence illuminates a path connecting plant molecular biology to Earth-system science

Albert Porcar-Castell[1*], Zbyněk Malenovský[2], Troy Magney[3], Shari Van Wittenberghe[1,4], Beatriz Fernández-Marín[5], Fabienne Maignan[6], Yongguang Zhang[7], Kadmiel Maseyk[8], Jon Atherton[1], Loren P. Albert[9, 10], Thomas Matthew Robson[11], Feng Zhao[12], Jose-Ignacio Garcia-Plazaola[13], Ingo Ensminger[14], Paulina A. Rajewicz[1], Steffen Grebe[15], Mikko Tikkanen[15], James R. Kellner[9, 16], Janne A. Ihalainen[17], Uwe Rascher[18], Barry Logan[19]

[1]Optics of Photosynthesis Laboratory, Institute for Atmospheric and Earth System Research/Forest Sciences, Viikki Plant Science Center, University of Helsinki, Helsinki, Finland.

[2]School of Geography, Planning, and Spatial Sciences, College of Sciences Engineering and Technology, University of Tasmania, Private Bag 76, Hobart, TAS 7001, Australia.

[3]Department of Plant Sciences, University of California, Davis. Davis, CA, 95616 United States of America.

[4]Laboratory of Earth Observation, University of Valencia, C/Catedrático José Beltrán, 2, 46980 Paterna, Spain.

[5]Department of Botany, Ecology and Plant Physiology, University of La Laguna (ULL), Tenerife 38200, Spain.

[6]Laboratoire des Sciences du Climat et de l'Environnement, LSCE/IPSL, CEA-CNRS-UVSQ, Université Paris-Saclay, Gif-sur-Yvette, France.

[7]International Institute for Earth System Sciences, Nanjing University, Nanjing, Jiangsu 210023, China.

[8]School of Environment, Earth and Ecosystem Sciences, The Open University, Milton Keynes MK7 6AA, United Kingdom.

[9]Institute at Brown for Environment and Society, Brown University, Providence, RI 02912, United States of America.

[10]Biology Department, West Virginia University, Morgantown, WV 26506-6300, United States of America.

[11]Organismal and Evolutionary Biology, Viikki Plant Science Centre (ViPS), Faculty of Biological and Environmental Science, 00014, University of Helsinki, Finland.

[12]School of Instrumentation Science and Opto-Electronics Engineering, Beihang University, Beijing, 100083, China.

[13]Department of Plant Biology and Ecology, University of the Basque Country (UPV/EHU), Bilbao, Spain.

[14]Department of Biology, Graduate Programs in Cell & Systems Biology and Ecology & Evolutionary Biology, University of Toronto, 3359 Mississauga Road, Mississauga, ON L5L 1C6, Canada.

[15]Molecular Plant Biology, University of Turku, FI-20520 Turku, Finland.

[16]Department of Ecology and Evolutionary Biology, Brown University, Providence RI 02912, United States of America.

[17]Nanoscience Center, Department of Biological and Environmental Science, University of Jyväskylä, Jyväskylä 40014, Finland.

[18]Institute of Bio- and Geosciences, Plant Sciences (IBG-2), Forschungszentrum Jülich GmbH, Jülich, Germany.

[19]Biology Department, Bowdoin College, Brunswick, Maine, United States of America.

For decades, the dynamic nature of chlorophyll-a fluorescence (ChlaF) has provided insight into the biophysics and ecophysiology of the light reactions of photosynthesis from the subcellular to leaf scales. Recent advances in remote sensing methods now enable detection of ChlaF induced by sunlight across a range of larger scales, using instruments mounted on towers above plant canopies to Earth-orbiting satellites. This signal is referred to as *solar-induced fluorescence* (SIF) and its application promises to overcome spatial constraints on studies of photosynthesis, opening new research directions and opportunities in ecology, ecophysiology, biogeochemistry, agriculture and forestry. However, to unleash the full potential of SIF, intensive cross-disciplinary work is required to harmonize these new advances with the rich history of biophysical and ecophysiological studies of ChlaF, fostering the development of next-generation plant physiological and Earth system models. Here, we introduce the scale-dependent link between SIF and photosynthesis, with an emphasis on seven remaining scientific challenges, and present a roadmap to facilitate future collaborative research towards new SIF applications.

When illuminated, chlorophyll-a molecules weakly emit light in the 650-850 nm range; that is, they fluoresce. Steady state[1-3] and time-resolved fluorescence spectroscopy[4-6], as well as pulse-amplitude modulated (PAM) fluorescence[7-9] have long been used by biophysicists, molecular biologists and ecophysiologists to elucidate the structure and function of the photosynthetic apparatus[10-14]. These techniques are regarded as active because the measured ChlaF originates from a controlled light source, and accordingly have largely[15,16] been restricted to measurements at the subcellular and leaf levels.

Interest in passive remote sensing methods capable of retrieving solar-induced ChlaF across a continuum of spatial scales emerged more than two decades ago[17-21]. These seminal activities led to the first demonstrations of tower-based[22,23] and satellite[24] SIF measurements over terrestrial ecosystems. The opportunity to remotely detect an energy flux (Box 1) that arises directly from

within the photosynthetic process spurred the rapid development of measurement techniques, retrieval protocols, and models for estimating and interpreting SIF across scales. As reviewed in Mohammed et al.[21] and Aasen et al.[25], SIF can now be measured from an expanding number of sensors mounted on towers[26,27], drones[28,29], aircraft[30,31] and satellites with ever-improving spatial and temporal resolution[32-35]. So far, all satellite SIF retrievals have been serendipitous, relying on instruments originally designed to measure atmospheric gases. The first satellite mission designed specifically for the measurement of SIF is the ESA FLuorescence EXplorer (FLEX) mission, which is set to launch in 2024[36].

SIF methods are rapidly breaking through the scale bottleneck of traditional ChlaF measurements, opening up a range of new opportunities to study photosynthesis across the continuum of spatial scales from the leaf, through plant canopies, and up to the globe. With SIF we now have the potential to illuminate the path connecting plant molecular biology to Earth-system science. However, before the full potential of multiscale SIF observations can be realized, a number of challenges must be overcome. Extracting the information embedded in the SIF signal requires a fundamental understanding and a quantitative description of the processes that connect measured ChlaF with photosynthesis (Fig.1), as well as their variation across space and time (Fig. 2). In this Perspective, we present these challenges and propose a roadmap of activities to facilitate future research. Finally, we discuss key emerging SIF applications that can benefit from cross-disciplinary expertise.

Challenge 1: $APAR_g$. The common denominator between ChlaF and the photosynthetic uptake of CO_2 is the flux of photosynthetically active radiation absorbed by photosynthetic pigments, or $APAR_g$ (where the g stands for green), which provides the foundation for the mechanistic connection between SIF and photosynthesis. $APAR_g$ is the product of the incoming photosynthetically active radiation (PAR) and the fraction of this PAR absorbed by photosynthetic pigments ($fAPAR_g$) (Fig.1). Importantly, although the absorption of radiation by leaves and plant

canopies can be quantified using radiometric sensors either coupled to an integrating sphere[37] (e.g. leaf absorptance profile in Fig.1) or mounted above and below a plant canopy[38], these measurements also include a significant and dynamic contribution from non-photosynthetic pigments and other canopy elements. While inaccuracies in the estimation of $APAR_g$ do not disrupt the relationship between SIF and photosynthesis, accurate quantification of the energy flux entering the photosynthetic process is essential for a mechanistic interpretation of SIF and remains a challenge.

Challenge 2: Distribution of excitation energy between PSII and PSI and their ChlaF emissions.

$APAR_g$ is absorbed mostly by chlorophyll-a and chlorophyll-b associated with either photosystem II (PSII) or photosystem I (PSI) reaction centres. Interestingly, while both types of chlorophyll have the capacity to fluoresce, essentially all chlorophyll fluorescence *in vivo* originates from chlorophyll-a due to the efficient and rapid transfer of excitation energy from chlorophyll-b to chlorophyll-a within light harvesting antennae[39]. Likewise, although both photosystems emit ChlaF, ChlaF from PSII typically dominates the signal, especially in the red region of the spectrum[3,40,41], and exhibits greater variation in quantum yield in response to photochemical and non-photochemical processes[10,13]. The dynamic nature of PSII ChlaF explains the widespread application of PAM fluorescence to probe the energy partitioning between photochemical and non-photochemical processes or to estimate the rate of linear electron transport (LET) in PSII[42]. However, critically, the estimation of LET requires knowledge of the distribution of absorption between the photosystems (i.e. the use of an energy partitioning factor), which is rarely measured and assumed instead to be 0.5[8]. Although biochemical and biophysical methods to assess the stoichiometry and antenna sizes of PSI and PSII do exist[43-46], these methods only provide a relative assessment of the energy distribution; absolute quantification requires the combination of simultaneous ChlaF to probe PSII with 820 nm absorption to probe PSI combined with photosynthetic gas exchange measurements[47,48]. Overall, the evidence gathered to date suggests that

neither the distribution of excitation energy between PSII and PSI nor the contribution of ChlaF from PSI to SIF remain constant over time, between species or within canopy light gradients. Questions remain: how large is this variability? What controls it? And what is its significance for the interpretation of SIF? Answers to these questions await the development of versatile field methods and protocols (e.g. based on rapid optical measurements[49]) to enable the characterization of these factors across a wide range of conditions.

Challenge 3: Energy partitioning in PSII. Energy absorbed in PSII is partitioned between three main processes: a) photochemical quenching (PQ) of excitation energy leading to linear electron transport, b) non-photochemical quenching (NPQ), which includes both regulated and sustained forms of thermal dissipation of excitation energy, and c) emission of ChlaF. Importantly, the rate constants of PQ and NPQ are highly dynamic, which allows plants to regulate the flow of energy through PSII and to protect against light-induced damage[50, 51]. During the growing season, rate constants vary over time-scales of seconds to minutes in response to the redox dynamics of the quinone acceptor pool and induction and relaxation of regulated thermal dissipation. Outside of the growing season, or during periods of profound environmental stress, rate constants can be affected by downregulation or photoinhibition of PQ and the induction of sustained NPQ. In contrast, the rate constant associated with fluorescence emission is widely assumed to remain constant. Accordingly, changes in the quantum yield of ChlaF (ΦF) reflect the combined effect of PQ and NPQ dynamics and a quantitative connection between ΦF and ΦP (the quantum yield of photochemistry) cannot be established without knowledge of either PQ or NPQ[12,52]. PAM fluorescence uses saturating light pulses to solve the energy partitioning and estimate ΦP; an approach that is not feasible during SIF measurements, precluding partitioning from SIF alone.

Under certain conditions, either NPQ or PQ can dominate the relationships between ΦF and ΦP, resulting in the emergence of a positive or negative relationship respectively. For example, under low light - when NPQ remains relatively stable - the relationship between ΦP and ΦF is negative

under the action of PQ, which exerts opposite effects on (i.e. decouples) ΦP and ΦF. Under high light - when PQ tends to saturate and remain stable - the relationship between ΦP and ΦF is positive under the action of NPQ, which competes for excitation with both (i.e. couples) ΦP and ΦF[12,52,53]. The latter case may explain the seasonal correlation between ΦP and ΦF observed at the leaf[54,55] (Fig. 2) and canopy scales[27], in response to the modulation of sustained NPQ that protects the foliage from the harmful combination of excessive light and low temperatures[56-58]. Despite the positive relationship between ΦP and ΦF that emerges in response to certain stress conditions, the quantitative treatment of the energy partitioning in PSII requires the use of mechanistic models and remains one of the core challenges to the interpretation of SIF[52,59,60].

Challenge 4: Alternative energy sinks. Photosynthetic linear electron transport provides reducing power for a range of metabolic processes beyond CO_2 assimilation via the Calvin cycle, including chlororespiration[61], photorespiration[62], nitrogen, sulphur and oxygen reduction (the latter known as the Mehler reaction in the water-water cycle[63]), and the synthesis of volatile organic compounds[64]. Importantly, the dynamics of these 'non-assimilatory' electron sinks can affect ChlF in a manner not directly correlated with CO_2 assimilation. In particular, because alternative energy sinks can have a protective function by sustaining LET under conditions when CO_2 assimilation is impaired[65,66], they could influence the capacity of SIF to detect certain plant stress responses. Therefore, it is critical to address the extent that these dynamics decouple SIF from GPP, in particular during plant stress responses. As with Challenge 2, answering this question will benefit from the development of versatile field methods and protocols to promote the widespread characterization of these factors across a wide range of conditions.

Challenge 5: Leaf and canopy ChlaF scattering, reabsorption and measurement geometry. Although the lighter and darker green stripes seen on a professional sports field may give the impression of different chlorophyll contents, they are an optical reflection effect created when the grass is bent in a particular direction during mowing. SIF measurements over plant canopies are

similarly affected by the distribution of leaves, canopy architecture and measurement geometry[38,67,68]. The amount and distribution of chlorophyll within a leaf (influenced by photosystem and thylakoid structure, chloroplast distribution, and internal leaf morphology), as well as the amount and geometrical arrangement of leaves and other non-photosynthetic material within a plant canopy (influenced by branch/stem architecture) drive $APAR_g$, connecting SIF and photosynthesis at the leaf and canopy scales, respectively. Once emitted, ChlaF photons travel through the same leaf and canopy structures, where some of the ChlaF photons are reabsorbed (Fig. 1 and Fig. 2 "spectral dynamics"). As a result, spatial and temporal variations in leaf biochemistry, leaf morphology, and canopy architecture, as well as foliage illumination and viewing geometry, influence the probability of ChlaF photons contributing to a SIF measurement (known as the escape probability, *f*esc). These factors decouple the total emitted ChlaF from the measured SIF, and by extension from photosynthesis. Radiative transfer models, which simulate the physical movement of photons through leaves and plant canopies (Box 2), can be used to provide a quantitative framework to investigate and account for the impact of these factors on $APAR_g$ and SIF observations[38,69]. Although spatially explicit RTM approaches are already available (see Supplementary Video 1 and 2), advances in the parametrization of within-leaf and canopy drivers of SIF - e.g. canopy gradients in foliar morphology, pigment contents (Challenge 1) or ChlaF contribution from PSI (Challenge 2)- remain areas of active development.

Challenge 6: Atmospheric absorption and scattering. Atmospheric gases, aerosols and other particles absorb and scatter ChlaF photons traveling from a plant canopy to a remote detector. The extent of atmospheric absorption and scattering of SIF depends on the retrieval wavelength, the distance between target and sensor, and the properties of the atmosphere (Box 1). In particular, SIF retrieval methods based on the in-filling of atmospheric gas absorption bands, such as the O2-A or O2-B bands (Fig. 1), face the challenge that the gas absorption feature used for the SIF retrieval simultaneously attenuates the ChlaF signal as it travels towards the detector. This effect requires a

correction even for short-distance measurements from canopy towers and drones[70]. Although an atmospheric RTM can be used to characterize and correct for these effects, its application requires site-specific measurements of atmospheric profile parameters for model input, which remains an operational challenge[71].

Challenge 7: Integrating SIF controls across space and time. A final challenge, and perhaps the most relevant, is the contextualization of the interpretation of SIF (including the previous six challenges) within the spatial and temporal domain of the measurements (Fig. 2). Temporally, ChlaF dynamics have been used to investigate the energy transfer within photosystems (femto-picosecond scale)[10,72], the redox status of the donor and acceptor sides of the photosystem (microsecond-millisecond scale)[4,5], and the variations in PQ and NPQ (seconds-to-seasonal scale)[50,51,58]. Spatially, the intensity and spectral properties of SIF are also controlled by factors that regulate both $APAR_g$ and ChlaF scattering and reabsorption within a leaf or plant canopy[73-75] (Fig. 2, "spectral dynamics"). When ChlaF is measured as SIF across coarser spatial and longer temporal scales, the signal carries information that aggregates an expanding assortment of physical and biological factors[53,76,77]. New controls may appear while the effects of others may be subordinated, strengthening (via 'couplers'; Fig. 2) or disrupting (via 'decouplers'; Fig. 2) the relationship between SIF and GPP.

For example, tower-based SIF studies reveal a strong seasonal linear relationship between canopy SIF and ecosystem GPP across a wide range of ecosystems[26,27,77], consistent with the coupling action of $APAR_g$ and NPQ described above. Yet, the sensitivity, strength and linearity of the seasonal SIF-GPP relationship is not universal and has been found to depend on additional physical and physiological decoupling factors, such as sun-vegetation-sensor geometries[78,79], vegetation canopy structure[67,80], or photosynthetic pathway (C3 vs. C4)[38,81], with contrasting responses to different environmental stressors[82,83]. Clearly, integrating and disentangling the relationship

between SIF and GPP across species, space, time and in response to environmental stress, remains still a challenge that calls for comprehensive field studies.

Roadmap towards a consistent interpretation of SIF

The time for multiscale SIF measurements is already here (Fig. 3). Yet, converting these data into meaningful information and new applications still requires effort dedicated to scaling and standardizing methods for SIF interpretation, with particular attention to the seven challenges described above. This process requires accounting for the influence of 1) instrumental, 2) atmospheric, 3) structural and 4) physiological factors to unlock the quantitative association between measured SIF and photosynthesis (Fig. 4). Addressing these challenges requires new data, protocols and models to interpret SIF and bridge the gap between molecular processes, i.e. photosynthesis, and satellite imagery.

At the leaf level, new instruments and techniques employing optical bandpass filters have been developed to record fluorescence spectral dynamics under both natural or controlled illumination, temperature, and CO_2 concentration[25,84-87]. Such spectral approaches, combined with foliar pigment analysis, photosynthetic gas exchange, and PAM ChlaF measurements, provide new insights into the connection between SIF and photosynthesis dynamics of leaves[55,85,88]. Going forward, mechanistically modeling the link between SIF and GPP (**Challenges 1-4)** will require the combination of field campaigns covering full growing seasons, multiple species and stress responses with detailed experimentation under highly controlled conditions, for example using *Arabidopsis* mutants with altered photochemical properties[14,89]. In particular, the development of versatile field instrumentation and protocols for the estimation of APARg (**Challenge 1**), energy distribution between PSII and PSI - including the ChlaF contribution from PSI - (**Challenge 2**), or the quantification of alternative energy sinks (**Challenge 4**), is key to resolving the spatial and temporal influences of these factors on SIF.

The synergistic use of complementary data streams can also help to constrain the modelling of photosynthesis and support SIF interpretation. For example, leaf and canopy reflectance data can inform us on the chlorophyll content in the leaf or the number of leaves in the canopy[90], relating to $APAR_g$ (**Challenge 1**). In addition, reflectance data have been used to explore the regulatory dynamics of NPQ[91], which could contribute to resolving energy partitioning in PSII (**Challenge 3**). This approach is feasible due to the spectral change in reflectance signature that accompanies the operation of the xanthophyll cycle[92] - by which violaxanthin is converted to antheraxanthin and zeaxanthin in a process that modulates NPQ[50,93] - as well as the seasonal dynamics in leaf carotenoid and chlorophyll contents[94]. These spectral changes, which have been captured by the photochemical reflectance index (PRI)[93,95,96] or the Chlorophyll/Carotenoid Index (CCI)[97], are now being revisited and investigated in depth across the whole VIS-NIR region alongside with SIF dynamics[87,92]. Clearly, as in the case of SIF, careful use of canopy and atmospheric RTMs will be needed to disentangle these subtle physiologically-induced reflectance changes from those of a dynamic background[71]. In addition to synergies with spectral reflectance, use of thermal imaging[98], radar[99], or multispectral laser scanning methods[100] offer interesting possibilities to constrain the carbon reactions of photosynthesis by providing independent information on plant water status supporting SIF interpretation (**Challenge 4**). Likewise, leaf and ecosystem-level measurements of carbonyl sulfide (COS) uptake by vegetation can provide an independent source of information on stomatal conductance in vascular plants[101], which could be highly relevant for the development and validation of ecosystem-level SIF-GPP models.

Process-based and radiative transfer models are required to integrate physical and physiological mechanisms operating at different scales (**Challenge 7**), providing excellent frameworks for multidisciplinary collaborations to connect molecular-level with Earth-system processes. Clearly, as our mechanistic understanding of the connection between SIF and GPP increases (**Challenges 1-4**), so will the accuracy of process-based models. For example, the integration of the Farquhar-

273 Caemmerer-Berry[102] biochemical model of photosynthesis into dynamic land-surface models (e.g.,
274 ORCHIDEE[103] or BETHY[104]) provides a gateway for assimilating satellite SIF data and improving
275 the accuracy of GPP estimations[105,106]. In addition, SIF resides at the core of a new generation of
276 photosynthesis models that emphasize the light reactions (Gu et al. 2019). In the case of RTMs
277 (Box 2) with established SIF capabilities, further improvements can be achieved by coupling with
278 new techniques measuring detailed 3D structures. Leaf RTMs would benefit from including
279 variations in leaf morphology, thylakoid structure, or the spectral signatures of PSI and PSII. The
280 3D parameterization of canopy RTMs via lidar-based reconstruction methods[78,107,108], coupled to
281 non-imaging[26,28] and imaging proximal/airborne SIF measurements (Fig. 3)[109-111], offers excellent
282 opportunities to integrate and resolve the diversity of factors that control SIF across space and time
283 (**Challenge 7**). Drone-based measurements could serve to investigate and model the impact of
284 atmospheric properties on SIF retrieval approaches, by hovering at different distances above the
285 target[70] (**Challenge 6**). Finally, less accurate but simpler alternative methods for separating the
286 physiological and structural influences on the SIF signal have been recently proposed based on the
287 theory of vegetation canopy near-infrared spectral invariants[112,113]. Whether this or other correction
288 methods are applicable to canopy SIF acquisitions across scales, especially observations at very
289 high spatial resolutions (Fig. 3) should be further investigated.

290 Equally critical for the consistent interpretation of SIF is the establishment of a global network and
291 database of leaf and ecosystem-level SIF measurements covering different biomes, and supporting
292 model development as well as airborne and satellite calibration/validation activities. While regional
293 SIF networks are starting to emerge in North America, Europe, and Asia, their global connectivity
294 should be a priority to promote the adoption of standards for instrument calibrations and long-term
295 monitoring operations (Fig. 4).

296 Our roadmap for resolving the seven SIF challenges will only succeed through multidisciplinary
297 collaboration involving specialists from across molecular biology, plant physiology, optical physics

298 and remote sensing. Together, the characterization and modeling of the interplay between structural,
299 optical and functional dynamics of leaves and plant canopies, can turn our crops and forests into
300 observable field laboratories.

301 **Emerging and potential SIF applications**

302 Satellite SIF data are already providing new insight into photosynthetic dynamics at the global
303 scale[114-117]. Likewise, with the advent of multiscale SIF measurements (Fig. 3), and as the
304 remaining challenges are overcome (Fig. 4), a new range of SIF applications is unfolding across
305 fields of biochemistry, biophysics, ecology, ecophysiology, biogeochemistry, agriculture and
306 forestry (Fig. 5). Equally important, the continuum of scales at which SIF can be measured provides
307 a focal point to promote and strengthen the interaction between research communities, from plant
308 molecular biology to Earth-system science. Here, we outline four examples of potential and
309 emerging SIF applications.

310 ***Spatial and 3D photosynthesis.*** Photosynthetic CO_2 assimilation can be measured using infra-red
311 gas analyzers, either coupled to chambers or enclosures at the leaf, shoot, and whole-plant level[118],
312 or with a sonic anemometer at the ecosystem level using the eddy covariance approach[119]. These
313 methods, however, lack detailed spatial information. Spatial measurements of photosynthesis, in
314 terms of photochemical rates of the light reactions, require the use of imaging systems that, to date,
315 have remained restricted to the scale of leaves or small-sized plants, e.g. PAM imaging methods[120].
316 SIF measurements have potential to fill this scale gap. For example, SIF imaging (Fig. 3) could be
317 benchmarked with eddy-covariance methods to reveal the spatial variability of photosynthesis
318 within the footprint of ecosystem eddy covariance measurements, allowing us to investigate the
319 influence of microenvironment, understory and vertical canopy structure, or the interplay between
320 biological and functional diversity within the ecosystem. Likewise, SIF imaging could be applied to

resolve photosynthesis dynamics in 3D, helping to advance our understanding of the interaction between plant structure and function[121,122].

Physiological phenotyping and pre-visual stress detection. Spatial and temporal variations in plant morphological traits (e.g., canopy height, leaf area, and plant growth) have been widely used as markers for field phenotypic variability and to investigate long-term plant stress responses. However, these traits are insufficiently responsive to rapid plant physiological changes. This makes them ill-suited for physiological phenotyping (i.e. breeding plant phenotypes displaying specific physiological responses to the environment), or pre-visual stress detection and subsequent optimization of water, pesticide and fertilizer use. The current phenotyping focus has, therefore, shifted towards measurements in the visible and infrared spectral ranges, where reflectance changes can be associated with specific physiological and biochemical traits[123] or used for early-stress detection[124]. In this context, emerging SIF imaging systems have already provided promising results for applications in precision agriculture and detection of pest infestations[109,125,126]. In the near future, these methods could also support precision forestry applications related to seedling production or tree-scale forest management.

Functional plant diversity and spatial ecology. Functional diversity is a fundamental component of the biodiversity concept[127]. As a global network for monitoring biodiversity through remotely sensed plant functional traits is being developed[128], SIF could become one of the new essential variables for mapping functional diversity across ecosystem and landscape scales, given the wide range of biochemical and physiological factors that SIF is sensitive to (Fig. 2) in relation to plant productivity. For example, SIF has been shown to convey spatial information on leaf mass and chlorophyll content[129], and other functional plant traits[130] in various forest ecosystems. Additionally and importantly, the combination of high-resolution structural, spectral and SIF data is potentially the only viable option to investigate ecosystem functions that have remained hidden from our observational abilities, such as photosynthetic phenology in evergreen forests[27], cryptogamic

346 biocrusts[131] and spatially fragmented Antarctic mosses[90]. Together with spatial photosynthesis, SIF
347 could also offer unique opportunities for studies in spatial ecology[110,131], where plant environmental
348 responses and biotic interactions could leave their imprint in SIF.

349 ***Carbon and water cycle studies.*** The carbon and water cycles of terrestrial ecosystems are
350 intricately connected via stomatal regulation and total leaf area. Because both canopy
351 evapotranspiration and canopy SIF dynamics are strongly controlled by leaf area, and since ChlaF
352 can also decrease with stomatal closure - via increased NPQ in response to water stress[132]; tower
353 and satellite SIF have been preliminarily used to investigate canopy conductance and plant
354 transpiration[133,134]. No doubt, better constraints on transpiration and photosynthetic dynamics in
355 land-surface models will be achieved as the mechanistic basis of SIF is elucidated across scales
356 (Challenges 1-7), and the integration of SIF with other remote sensing datasets increases, such as
357 land-surface temperature[133,135], surface soil moisture[106], radar-measured vegetation optical depth
358 characterizing canopy structure and water content[136,137], or column-averaged atmospheric CO_2 [138].
359 New knowledge of photosynthesis at the ecosystem and regional scales will bring further insight
360 into the large-scale interactions between environmental drivers and plant productivity, and
361 feedbacks between the biosphere and atmosphere.

362 **Concluding remarks**

363 The SIF signal gathers a wealth of physiological, biochemical, and structural information as it
364 travels from the photosystems to the top of canopy and beyond (Fig. 2). This can leave the
365 impression that SIF is, to use the classic analogy, the 'Swiss army knife' of photosynthesis
366 measurements. Critically, the variation in SIF caused by physical and biotic factors is entangled in
367 the spatiotemporal domain, and our capacity to disentangle it into useful informative components
368 requires further attention. Historically, photosynthesis research has been a multidisciplinary
369 endeavor, with breakthroughs in the 20th century emerging from collaboration between chemists,

biologists and physicists. We are now entering a new era of multiscale observations of photosynthesis which requires the interdisciplinary research environment to flourish further, this time to resolve the mechanistic connection between SIF and GPP and to scale it across space and time. The technology to measure SIF is developing at a faster pace than our capacity to interpret the acquired data. With the challenges, roadmap and unfolding opportunities introduced here we hope to encourage more scientists to join the multidisciplinary quest to reveal the true potential of SIF observation.

References

1. Genty, B., Wonders, J. & Baker, N. R. Non-photochemical quenching of Fo in leaves is emission wavelength dependent: consequences for quenching analysis and its interpretation. *Photosynth. Res.* **26**, 133-139 (1990).

2. Lichtenthaler, H. K., Wenzel, O., Buschmann, C. & Gitelson, A. Plant Stress Detection by Reflectance and Fluorescence a. *Ann. N. Y. Acad. Sci.* **851**, 271-285 (1998).

3. Franck, F., Juneau, P. & Popovic, R. Resolution of the photosystem I and photosystem II contributions to chlorophyll fluorescence of intact leaves at room temperature. *Biochim. Biophys. Acta-Bioenergetics* **1556**, 239-246 (2002).

4. Neubauer, C. & Schreiber, U. The polyphasic rise of chlorophyll fluorescence upon onset of strong continuous illumination: I. Saturation characteristics and partial control by the photosystem II acceptor side. *Zeitschrift für Naturforschung C* **42**, 1246-1254 (1987).

5. Strasser, R. J., Tsimilli-Michael, M. & Srivastava, A. Analysis of the chlorophyll a fluorescence transient. In: Papageorgiou G.C., Govindjee (eds) Chlorophyll a Fluorescence. Advances in Photosynthesis and Respiration, vol 19. Springer, Dordrecht (2004).

6. Ihalainen, J. A. *et al*. Kinetics of excitation trapping in intact photosystem I of Chlamydomonas reinhardtii and Arabidopsis thaliana. *Biochim. Biophys. Acta-Bioenergetics* **1706**, 267-275 (2005).

7. Schreiber, U., Schliwa, U. & Bilger, W. Continuous recording of photochemical and non-photochemical chlorophyll fluorescence quenching with a new type of modulation fluorometer. *Photosynth. Res.* **10**, 51-62 (1986).

8. Maxwell, K. & Johnson, G. N. Chlorophyll fluorescence—a practical guide. *J. Exp. Bot.* **51**, 659-668 (2000).

9. Baker, N. R. Chlorophyll fluorescence: a probe of photosynthesis in vivo. *Annu.Rev.Plant Biol.* **59**, 89-113 (2008).

10. Govindjee, E. 63 Years since Kautsky-chlorophyll-a fluorescence. *Aust. J. Plant Physiol.* **22**, 131-160 (1995).

11. Kalaji, H. M. *et al*. Frequently asked questions about in vivo chlorophyll fluorescence: practical issues. *Photosynth. Res.* **122**, 121-158 (2014).

12. Porcar-Castell, A. *et al*. Linking chlorophyll a fluorescence to photosynthesis for remote sensing applications: mechanisms and challenges. *J. Exp. Bot.* **65**, 4065-4095 (2014).

13. Kalaji, H. M. *et al*. Frequently asked questions about chlorophyll fluorescence, the sequel. *Photosynth. Res.* **132**, 13-66 (2017).

14. Tikkanen, M., Rantala, S., Grieco, M. & Aro, E. Comparative analysis of mutant plants impaired in the main regulatory mechanisms of photosynthetic light reactions-From biophysical measurements to molecular mechanisms. *Plant Physiol. Biochem.* **112**, 290-301 (2017).

15. Kolber, Z. *et al*. Measuring photosynthetic parameters at a distance: laser induced fluorescence transient (LIFT) method for remote measurements of photosynthesis in terrestrial vegetation. *Photosynth. Res.* **84**, 121-129 (2005).

16. Keller, B. *et al*. Genotype specific photosynthesis x environment interactions captured by automated fluorescence canopy scans over two fluctuating growing seasons. *Front. Plant Sci.* **10**, 1482 (2019).

~~17. Buschmann, C., Nagel, E., Szabó, K. & Kocsányi, L. Spectrometer for fast measurements of in vivo reflectance, absorptance, and fluorescence in the visible and near-infrared. *Remote Sens. Environ.* **48**, 18-24 (1994).~~

~~18. Cecchi, G. *et al*. Remote sensing of chlorophyll a fluorescence of vegetation canopies: 1. Near and far field measurement techniques. *Remote Sens. Environ.* **47**, 18-28 (1994).~~

~~19. Davidson, M. *et al*. Mapping photosynthesis from space-a new vegetation fluorescence technique. *ESA Bulletin* **116**, 34-37 (2003).~~

~~20. Moya, I. *et al*. A new instrument for passive remote sensing: 1. Measurements of sunlight-induced chlorophyll fluorescence. *Remote Sens. Environ.* **91**, 186-197 (2004).~~

21. Mohammed, G. H. *et al*. Remote sensing of solar-induced chlorophyll fluorescence (SIF) in vegetation: 50 years of progress. *Remote Sens. Environ.* **231**, 111177 (2019).

22. Evain, S., Camenen, L. & Moya, I. Three-channel detector for remote sensing of chlorophyll fluorescence and reflectance from vegetation. In: M. Leroy (ed.), 8th International symposium: physical measurements and signatures in remote sensing, pp. 395-400. Aussois, CNES, France (2001).

23. Louis, J. *et al*. Remote sensing of sunlight-induced chlorophyll fluorescence and reflectance of Scots pine in the boreal forest during spring recovery. *Remote Sens. Environ.* **96**, 37-48 (2005).

24. Guanter, L. *et al*. Estimation of solar-induced vegetation fluorescence from space measurements. *Geophys. Res. Lett.* **34** (2007).

25. Aasen, H. *et al*. Sun-induced chlorophyll fluorescence II: review of passive measurement setups, protocols, and their application at the leaf to canopy level. *Remote Sensing* **11**, 927 (2019).

26. Yang, X. *et al*. Solar-induced chlorophyll fluorescence that correlates with canopy photosynthesis on diurnal and seasonal scales in a temperate deciduous forest. *Geophys. Res. Lett.* **42**, 2977-2987 (2015).

27. Magney, T. S. *et al*. Mechanistic evidence for tracking the seasonality of photosynthesis with solar-induced fluorescence. *PNAS* **116**, 11640-11645 (2019).

28. Bendig, J., Malenovský, Z., Gautam, D. & Lucieer, A. Solar-Induced Chlorophyll Fluorescence Measured From an Unmanned Aircraft System: Sensor Etaloning and Platform Motion Correction. *IEEE Trans. Geosci. Remote Sens.* (2019).

29. Vargas, J. Q. *et al*. Unmanned aerial systems (UAS)-based methods for solar induced chlorophyll fluorescence (SIF) retrieval with non-imaging spectrometers: state of the art. *Remote Sens.* **12**, 1624 (2020).

30. Rascher, U. *et al*. Sun-induced fluorescence–a new probe of photosynthesis: First maps from the imaging spectrometer HyPlant. *Global Change Biol.* **21**, 4673-4684 (2015).

31. Frankenberg, C. *et al*. The Chlorophyll Fluorescence Imaging Spectrometer (CFIS), mapping far red fluorescence from aircraft. *Remote Sens. Environ.* **217**, 523-536 (2018).

32. Frankenberg, C. *et al*. New global observations of the terrestrial carbon cycle from GOSAT: Patterns of plant fluorescence with gross primary productivity. *Geophys. Res. Lett.* **38** (2011).

~~33. Joiner, J. *et al.* Filling-in of broad far-red solar lines by terrestrial fluorescence and atmospheric Raman scattering as detected by SCIAMACHY satellite measurements. *Atmos. Meas. Tech.* **4**, 6185-6228 (2012).~~

~~34. Sun, Y. *et al*. Overview of Solar-Induced chlorophyll Fluorescence (SIF) from the Orbiting Carbon Observatory-2: Retrieval, cross-mission comparison, and global monitoring for GPP. *Remote Sens. Environ.* **209**, 808-823 (2018).~~

35. Köhler, P. *et al*. Global Retrievals of Solar-Induced Chlorophyll Fluorescence at Red Wavelengths With TROPOMI. *Geophys. Res. Lett.* **47**, e2020GL087541 (2020).

36. Drusch, M. *et al*. The fluorescence explorer mission concept - ESA's earth explorer 8. *IEEE Trans. Geosci. Remote Sens.* **55**, 1273-1284 (2016).

37. Olascoaga, B., Mac Arthur, A., Atherton, J. & Porcar-Castell, A. A comparison of methods to estimate photosynthetic light absorption in leaves with contrasting morphology. *Tree Physiol.* **36**, 368-379 (2016).

38. Zhang, Z. *et al*. Assessing bi-directional effects on the diurnal cycle of measured solar-induced chlorophyll fluorescence in crop canopies. *Agric. For. Meteorol.* **295**, 108147 (2020).

39. Bittner, T., Irrgang, K., Renger, G. & Wasielewski, M. R. Ultrafast excitation energy transfer and exciton-exciton annihilation processes in isolated light harvesting complexes of photosystem II (LHC II) from spinach. *J. Phys. Chem.* **98**, 11821-11826 (1994).

40. Pfündel, E. Estimating the contribution of photosystem I to total leaf chlorophyll fluorescence. *Photosynthesis Res.* **56**, 185-195 (1998).

41. Peterson, R. B. *et al*. Fluorescence Fo of photosystems II and I in developing C3 and C4 leaves, and implications on regulation of excitation balance. *Photosynth. Res.* **122**, 41-56 (2014).

42. Genty, B., Briantais, J. & Baker, N. R. The relationship between the quantum yield of photosynthetic electron transport and quenching of chlorophyll fluorescence. *Biochim. Biophys. Acta-General Subjects* **990**, 87-92 (1989).

43. Anderson, J. M., Chow, W. S. & Goodchild, D. J. Thylakoid membrane organisation in sun/shade acclimation. *Funct. Plant Biol.* **15**, 11-26 (1988).

44. Ballottari, M., Dall'Osto, L., Morosinotto, T. & Bassi, R. Contrasting behavior of higher plant photosystem I and II antenna systems during acclimation. *J. Biol. Chem.* **282**, 8947-8958 (2007).

45. Schreiber, U., Klughammer, C. & Kolbowski, J. Assessment of wavelength-dependent parameters of photosynthetic electron transport with a new type of multi-color PAM chlorophyll fluorometer. *Photosynth. Res.* **113**, 127-144 (2012).

~~46. Kou, J., Takahashi, S., Fan, D., Badger, M. R. & Chow, W. S. Partially dissecting the steady-state electron fluxes in Photosystem I in wild-type and pgr5 and ndh mutants of Arabidopsis. *Front. Plant Sci.* **6**, 758 (2015).~~

~~47. Laisk, A. & Loreto, F. Determining photosynthetic parameters from leaf CO_2 exchange and chlorophyll fluorescence (ribulose-1, 5-bisphosphate carboxylase/oxygenase specificity factor, dark respiration in the light, excitation distribution between photosystems, alternative electron transport rate, and mesophyll diffusion resistance. *Plant Physiol.* **110**, 903-912 (1996).~~

48. Laisk, A. *et al*. A computer-operated routine of gas exchange and optical measurements to diagnose photosynthetic apparatus in leaves. *Plant, Cell Environ.* **25**, 923-943 (2002).

49. Pfündel, E. E. Simultaneously measuring pulse-amplitude-modulated (PAM) chlorophyll fluorescence of leaves at wavelengths shorter and longer than 700 nm. *Photosynth. Res.*, 1-14 (2021).

50. Demmig-Adams, B. & Adams III, W. W. Photoprotection in an ecological context: the remarkable complexity of thermal energy dissipation. *New Phytol.* **172**, 11-21 (2006).

51. Porcar-Castell, A. A high-resolution portrait of the annual dynamics of photochemical and non-photochemical quenching in needles of Pinus sylvestris. *Physiol. Plant.* **143**, 139-153 (2011).

52. Van der Tol, C., Berry, J. A., Campbell, P. & Rascher, U. Models of fluorescence and photosynthesis for interpreting measurements of solar-induced chlorophyll fluorescence. *J. Geophys. Res.: Biogeosciences* **119**, 2312-2327 (2014).

53. Magney, T. S., Barnes, M. L. & Yang, X. On the covariation of chlorophyll fluorescence and photosynthesis across scales. *Geophys. Res. Lett.* **47**, e2020GL091098 (2020).

54. Springer, K. R., Wang, R. & Gamon, J. A. Parallel seasonal patterns of photosynthesis, fluorescence, and reflectance indices in boreal trees. *Remote Sens.* **9**, 691 (2017).

512 55. Zhang, C. *et al*. Do all chlorophyll fluorescence emission wavelengths capture the spring
513 recovery of photosynthesis in boreal evergreen foliage? *Plant, Cell Environ.* **42**, 3264-3279 (2019).

514 ~~56. Adams, W. W., Zarter, C. R., Ebbert, V. & Demmig-Adams, B. Photoprotective strategies of~~
515 ~~overwintering evergreens. *Bioscience* **54**, 41-49 (2004).~~

516 57. Ensminger, I. *et al*. Intermittent low temperatures constrain spring recovery of photosynthesis in
517 boreal Scots pine forests. *Glob. Change Biol.* **10**, 995-1008 (2004).

518 58. Verhoeven, A. Sustained energy dissipation in winter evergreens. *New Phytol.* **201**, 57-65
519 (2014).

520 59. Gu, L., Han, J., Wood, J. D., Chang, C. Y. & Sun, Y. Sun-induced Chl fluorescence and its
521 importance for biophysical modeling of photosynthesis based on light reactions. *New Phytol.* **223**,
522 1179-1191 (2019).

523 60. Raczka, B. *et al*. Sustained nonphotochemical quenching shapes the seasonal pattern of solar-
524 induced fluorescence at a high-elevation evergreen forest. *J. Geophys. Res.: Biogeosciences* **124**,
525 2005-2020 (2019).

526 61. Nixon, P. J. Chlororespiration. *Philos. Trans. R. Soc. Lond., B, Biol. Sci.* **355**, 1541-1547
527 (2000).

528 62. Ogren, W. L. Photorespiration: pathways, regulation, and modification. *Annu. Rev. Plant*
529 *Physiol.* **35**, 415-442 (1984).

530 63. Asada, K. The water-water cycle in chloroplasts: scavenging of active oxygens and dissipation
531 of excess photons. *Annu. Rev. Plant Biol.* **50**, 601-639 (1999).

64. Morfopoulos, C. *et al*. A model of plant isoprene emission based on available reducing power captures responses to atmospheric CO2. *New Phytol.* **203**, 125-139 (2014).

65. Laureau, C. *et al*. Plastid terminal oxidase (PTOX) has the potential to act as a safety valve for excess excitation energy in the alpine plant species R anunculus glacialis L. *Plant, Cell Environ.* **36**, 1296-1310 (2013).

66. Maseyk, K., Lin, T., Cochavi, A., Schwartz, A. & Yakir, D. Quantification of leaf-scale light energy allocation and photoprotection processes in a Mediterranean pine forest under extensive seasonal drought. *Tree Physiol.* **39**, 1767-1782 (2019).

67. Migliavacca, M. *et al*. Plant functional traits and canopy structure control the relationship between photosynthetic CO_2 uptake and far-red sun-induced fluorescence in a Mediterranean grassland under different nutrient availability. *New Phytol.* **214**, 1078-1091 (2017).

68. Biriukova, K. *et al*. Effects of varying solar-view geometry and canopy structure on solar-induced chlorophyll fluorescence and PRI. *Int. J. Appl. Earth. Obs. Geoinf.* **89**, 102069 (2020).

69. Kallel, A. FluLCVRT: Reflectance and fluorescence of leaf and canopy modeling based on Monte Carlo vector radiative transfer simulation. *J. Quant. Spectrosc. Radiat. Transf.* **253**, 107183 (2020).

70. Sabater, N. *et al*. Compensation of oxygen transmittance effects for proximal sensing retrieval of canopy–leaving sun–induced chlorophyll fluorescence. *Remote Sens.* **10**, 1551 (2018).

71. Sabater, N., Kolmonen, P., Van Wittenberghe, S., Arola, A. & Moreno, J. Challenges in the atmospheric characterization for the retrieval of spectrally resolved fluorescence and PRI region dynamics from space. *Remote Sens. Environ.* **254**, 112226 (2021).

553 72. Iermak, I., Vink, J., Bader, A. N., Wientjes, E. & van Amerongen, H. Visualizing heterogeneity
554 of photosynthetic properties of plant leaves with two-photon fluorescence lifetime imaging
555 microscopy. *Biochim. Biophys. Acta-Bioenergetics* **1857**, 1473-1478 (2016).

556 ~~73. Buschmann, C. & Lichtenthaler, H. K. Principles and characteristics of multi-colour~~
557 ~~fluorescence imaging of plants. *J. Plant Physiol.* **152**, 297-314 (1998).~~

558 74. Romero, J. M., Cordon, G. B. & Lagorio, M. G. Modeling re-absorption of fluorescence from
559 the leaf to the canopy level. *Remote Sens. Environ.* **204**, 138-146 (2018).

560 75. Magney, T. S. *et al*. Disentangling changes in the spectral shape of chlorophyll fluorescence:
561 Implications for remote sensing of photosynthesis. *J. Geophys. Res.: Biogeosciences* **124**, 1491-
562 1507 (2019).

563 76. Murchie, E. H. *et al*. Measuring the dynamic photosynthome. *Ann. Bot.* **122**, 207-220 (2018).

564 77. Yang, P., van der Tol, C., Campbell, P. K. & Middleton, E. M. Unraveling the physical and
565 physiological basis for the solar-induced chlorophyll fluorescence and photosynthesis relationship
566 using continuous leaf and canopy measurements of a corn crop. *Biogeosciences* **18**, 441-465 (2021).

567 78. Liu, X. *et al*. Downscaling of solar-induced chlorophyll fluorescence from canopy level to
568 photosystem level using a random forest model. *Remote Sens. Environ.* **231**, 110772 (2019).

569 79. Joiner, J. *et al*. Systematic Orbital Geometry-Dependent Variations in Satellite Solar-Induced
570 Fluorescence (SIF) Retrievals. *Remote Sens.***12**, 2346 (2020).

571 80. Dechant, B. *et al*. Canopy structure explains the relationship between photosynthesis and sun-
572 induced chlorophyll fluorescence in crops. *Remote Sens. Environ.* **241**, 111733 (2020).

81. He, L. *et al*. From the Ground to Space: Using Solar-Induced Chlorophyll Fluorescence to Estimate Crop Productivity. *Geophys. Res. Lett.* **47**, e2020GL087474 (2020).

82. Ač, A. *et al*. Meta-analysis assessing potential of steady-state chlorophyll fluorescence for remote sensing detection of plant water, temperature and nitrogen stress. *Remote Sens. Environ.* **168**, 420-436 (2015).

83. Wohlfahrt, G. *et al*. Sun-induced fluorescence and gross primary productivity during a heat wave. *Sci. Rep.* **8**, 1-9 (2018).

84. Van Wittenberghe, S., Alonso, L., Verrelst, J., Moreno, J. & Samson, R. Bidirectional sun-induced chlorophyll fluorescence emission is influenced by leaf structure and light scattering properties: A bottom-up approach. *Remote Sens. Environ.* **158**, 169-179 (2015).

85. Magney, T. S. *et al*. Connecting active to passive fluorescence with photosynthesis: A method for evaluating remote sensing measurements of Chl fluorescence. *New Phytol.* **215**, 1594-1608 (2017).

86. Rajewicz, P. A., Atherton, J., Alonso, L. & Porcar-Castell, A. Leaf-level spectral fluorescence measurements: comparing methodologies for broadleaves and needles. *Remote Sens.* **11**, 532 (2019).

87. Van Wittenberghe, S., Alonso, L., Malenovský, Z. & Moreno, J. In vivo photoprotection mechanisms observed from leaf spectral absorbance changes showing VIS-NIR slow-induced conformational pigment bed changes. *Photosynth. Res.* **142**, 283-305 (2019).

88. Meeker, E. W., Magney, T. S., Bambach, N., Momayyezi, M. & McElrone, A. J. Modification of a gas exchange system to measure active and passive chlorophyll fluorescence simultaneously under field conditions. *AoB Plants* **13**, plaa066 (2021).

595 89. Acebron, K. *et al*. Diurnal dynamics of nonphotochemical quenching in Arabidopsis npq
596 mutants assessed by solar-induced fluorescence and reflectance measurements in the field. *New*
597 *Phytol.* (2020).

598 90. Malenovský, Z., Lucieer, A., King, D. H., Turnbull, J. D. & Robinson, S. A. Unmanned aircraft
599 system advances health mapping of fragile polar vegetation. *Methods Ecol. Evol.* **8**, 1842-1857
600 (2017).

601 91. Atherton, J., Nichol, C. J. & Porcar-Castell, A. Using spectral chlorophyll fluorescence and the
602 photochemical reflectance index to predict physiological dynamics. *Remote Sens. Environ.* **176**, 17-
603 30 (2016).

604 92. Van Wittenberghe, S. *et al*. Combined dynamics of the 500–600 nm leaf absorption and
605 chlorophyll fluorescence changes in vivo: Evidence for the multifunctional energy quenching role
606 of xanthophylls. *Biochim. Biophys. Acta-Bioenergetics* **1862**, 148351 (2021).

607 93. Gamon, J. A. *et al*. Remote sensing of the xanthophyll cycle and chlorophyll fluorescence in
608 sunflower leaves and canopies. *Oecologia* **85**, 1-7 (1990).

609 94. Filella, I. *et al*. PRI assessment of long-term changes in carotenoids/chlorophyll ratio and short-
610 term changes in de-epoxidation state of the xanthophyll cycle. *Int. J. Remote Sens.* **30**, 4443-4455
611 (2009).

612 95. Peñuelas, J., Filella, I. & Gamon, J. A. Assessment of photosynthetic radiation-use efficiency
613 with spectral reflectance. *New Phytol.* **131**, 291-296 (1995).

614 96. Garbulsky, M. F., Peñuelas, J., Gamon, J., Inoue, Y. & Filella, I. The photochemical reflectance
615 index (PRI) and the remote sensing of leaf, canopy and ecosystem radiation use efficiencies: A
616 review and meta-analysis. *Remote Sens. Environ.* **115**, 281-297 (2011).

617 97. Gamon, J. A. *et al*. A remotely sensed pigment index reveals photosynthetic phenology in
618 evergreen conifers. *PNAS* **113**, 13087-13092 (2016).

619 98. Costa, J. M., Grant, O. M. & Chaves, M. M. Thermography to explore plant-environment
620 interactions. *J. Exp. Bot.* **64**, 3937-3949 (2013).

621 99. Konings, A. G., Rao, K. & Steele-Dunne, S. C. Macro to micro: microwave remote sensing of
622 plant water content for physiology and ecology. *New Phytol.* **223**, 1166-1172 (2019).

623 100. Junttila, S. *et al*. Terrestrial laser scanning intensity captures diurnal variation in leaf water
624 potential. *Remote Sens. Environ.* **255**, 112274 (2021).

625 101. Whelan, M. E. *et al*. Two Scientific Communities Striving for a Common Cause: innovations
626 in carbon cycle science. *Bull. Am. Meteorol. Soc.* (2020).

627 102. Farquhar, G. D., von Caemmerer, S. v. & Berry, J. A. A biochemical model of photosynthetic
628 CO 2 assimilation in leaves of C 3 species. *Planta* **149**, 78-90 (1980).

629 103. Bacour, C. *et al*. Improving estimates of gross primary productivity by assimilating solar-
630 induced fluorescence satellite retrievals in a terrestrial biosphere model using a process-based SIF
631 model. *J. Geophys. Res.: Biogeosciences* **124**, 3281-3306 (2019).

632 104. Norton, A. J. *et al*. Estimating global gross primary productivity using chlorophyll
633 fluorescence and a data assimilation system with the BETHY-SCOPE model. *Biogeosciences* **16**,
634 3069-3093 (2019).

635 105. Thum, T. *et al*. Modelling sun-induced fluorescence and photosynthesis with a land surface
636 model at local and regional scales in northern Europe. *Biogeosciences* **14**, 1969-1987 (2017).

637 106. Qiu, B., Chen, J. M., Ju, W., Zhang, Q. & Zhang, Y. Simulating emission and scattering of
638 solar-induced chlorophyll fluorescence at far-red band in global vegetation with different canopy
639 structures. *Remote Sens. Environ.* **233**, 111373 (2019).

640 107. Janoutová, R. *et al*. Influence of 3D spruce tree representation on accuracy of airborne and
641 satellite forest reflectance simulated in DART. *Forests* **10**, 292 (2019).

642 ~~108. Wallace, L., Lucieer, A., Malenovský, Z., Turner, D. & Vopěnka, P. Assessment of forest~~
643 ~~structure using two UAV techniques: A comparison of airborne laser scanning and structure from~~
644 ~~motion (SfM) point clouds. *Forests* 7, 62 (2016).~~

645 109. Pinto, F. *et al*. Sun-induced chlorophyll fluorescence from high-resolution imaging
646 spectroscopy data to quantify spatio-temporal patterns of photosynthetic function in crop canopies.
647 *Plant, Cell Environ.* **39**, 1500-1512 (2016).

648 110. Kellner, J. R., Albert, L. P., Burley, J. T. & Cushman, K. C. The case for remote sensing of
649 individual plants. *Am. J. Bot.* **106**, 1139-1142 (2019).

650 111. Siegmann, B. *et al*. The high-performance airborne imaging spectrometer HyPlant—From raw
651 images to top-of-canopy reflectance and fluorescence products: Introduction of an automatized
652 processing chain. *Remote Sens.* **11**, 2760 (2019).

653 112. Yang, P., van der Tol, C., Campbell, P. K. & Middleton, E. M. Fluorescence Correction
654 Vegetation Index (FCVI): A physically based reflectance index to separate physiological and non-
655 physiological information in far-red sun-induced chlorophyll fluorescence. *Remote Sens. Environ.*
656 **240**, 111676 (2020).

657 113. Zeng, Y. *et al*. A radiative transfer model for solar induced fluorescence using spectral
658 invariants theory. *Remote Sens. Environ.* **240**, 111678 (2020).

659 114. Guanter, L. *et al*. Global and time-resolved monitoring of crop photosynthesis with chlorophyll
660 fluorescence. *PNAS* **111**, E1327-E1333 (2014).

661 115. Bond-Lamberty, B., Bailey, V. L., Chen, M., Gough, C. M. & Vargas, R. Globally rising soil
662 heterotrophic respiration over recent decades. *Nature* **560**, 80-83 (2018).

663 116. Green, J. K. *et al*. Large influence of soil moisture on long-term terrestrial carbon uptake.
664 *Nature* **565**, 476 (2019).

665 117. Wang, S. *et al*. Urban− rural gradients reveal joint control of elevated CO 2 and temperature
666 on extended photosynthetic seasons. *Nat. Ecol. Evo.* **3**, 1076-1085 (2019).

667 118. Long, S. P., Farage, P. K. & Garcia, R. L. Measurement of leaf and canopy photosynthetic
668 CO2 exchange in the field. *J. Exp. Bot.* **47**, 1629-1642 (1996).

669 119. Baldocchi, D. D. Assessing the eddy covariance technique for evaluating carbon dioxide
670 exchange rates of ecosystems: past, present and future. *Glob. Change Biol.* **9**, 479-492 (2003).

671 120. Kaiser, Y. I., Menegat, A. & Gerhards, R. Chlorophyll fluorescence imaging: a new method
672 for rapid detection of herbicide resistance in A lopecurus myosuroides. *Weed Res.* **53**, 399-406
673 (2013).

674 121. Sievänen, R., Godin, C., DeJong, T. M. & Nikinmaa, E. Functional–structural plant models: a
675 growing paradigm for plant studies. *Ann. Bot.* **114**, 599-603 (2014).

676 122. Damm, A., Paul-Limoges, E., Kükenbrink, D., Bachofen, C. & Morsdorf, F. Remote sensing
677 of forest gas exchange: Considerations derived from a tomographic perspective. *Glob. Change Biol.*
678 **26**, 2717-2727 (2020).

123. Ensminger, I. Fast track diagnostics: Hyperspectral reflectance differentiates disease from drought stress in trees. *Tree Physiol.* **40**, 1143-1146 (2020).

124. Mutka, A. M. & Bart, R. S. Image-based phenotyping of plant disease symptoms. *Frontiers in plant science* **5**, 734 (2015).

~~125. Hernández-Clemente, R., North, P. R., Hornero, A. & Zarco-Tejada, P. J. Assessing the effects of forest health on sun-induced chlorophyll fluorescence using the FluorFLIGHT 3-D radiative transfer model to account for forest structure. *Remote Sens. Environ.* **193**, 165-179 (2017).~~

126. Zarco-Tejada, P. J. *et al*. Previsual symptoms of Xylella fastidiosa infection revealed in spectral plant-trait alterations. *Nat. Plants* **4**, 432-439 (2018).

127. Díaz, S. & Cabido, M. Vive la différence: plant functional diversity matters to ecosystem processes. *Trends Ecol. Evol.* **16**, 646-655 (2001).

128. Skidmore, A. K. *et al*. Environmental science: Agree on biodiversity metrics to track from space. *Nat. News* **523**, 403 (2015).

129. Tagliabue, G. *et al*. Sun–induced fluorescence heterogeneity as a measure of functional diversity. *Remote Sens. Environ.* **247**, 111934 (2020).

130. Pacheco-Labrador, J. *et al*. Multiple-constraint inversion of SCOPE. Evaluating the potential of GPP and SIF for the retrieval of plant functional traits. *Remote Sens. Environ.* **234**, 111362 (2019).

131. Smith, W. K. *et al*. Remote sensing of dryland ecosystem structure and function: Progress, challenges, and opportunities. *Remote Sens. Environ.* **233**, 111401 (2019).

132. Flexas, J. *et al*. Steady-state chlorophyll fluorescence (Fs) measurements as a tool to follow variations of net CO2 assimilation and stomatal conductance during water-stress in C3 plants. *Physiol. Plant.* **114**, 231-240 (2002).

133. Maes, W. H. *et al*. Sun-induced fluorescence closely linked to ecosystem transpiration as evidenced by satellite data and radiative transfer models. *Remote Sens. Environ.* **249**, 112030 (2020).

134. Shan, N. *et al*. A model for estimating transpiration from remotely sensed solar-induced chlorophyll fluorescence. *Remote Sens. Environ.* **252**, 112134 (2021).

~~135. Pagán, B. R., Maes, W. H., Gentine, P., Martens, B. & Miralles, D. G. Exploring the potential of satellite solar-induced fluorescence to constrain global transpiration estimates. *Remote Sens.* **11**, 413 (2019).~~

~~136. Teubner, I. E. *et al*. Assessing the relationship between microwave vegetation optical depth and gross primary production. *Int. J. Appl. Earth. Obs. Geoinf.* **65**, 79-91 (2018).~~

137. Wang, X. *et al*. Globally consistent patterns of asynchrony in vegetation phenology derived from optical, microwave, and fluorescence satellite data. *J. Geophys. Res.: Biogeosciences* **125**, e2020JG005732 (2020).

138. Liu, W. *et al*. Simulating solar-induced chlorophyll fluorescence in a boreal forest stand reconstructed from terrestrial laser scanning measurements. *Remote Sens. Environ.* **232**, 111274 (2019).

139. Albert, L. P. *et al.* Stray light characterization in a high-resolution imaging spectrometer designed for solar-induced fluorescence. Proc. SPIE 10986, Algorithms, Technologies, and Applications for Multispectral and Hyperspectral Imagery XXV, 109860G (2019).

140. Meroni, M. *et al*. Remote sensing of solar-induced chlorophyll fluorescence: Review of methods and applications. *Remote Sens. Environ.* **113**, 2037-2051 (2009).

141. Cendrero-Mateo, M. P. *et al*. Sun-induced chlorophyll fluorescence III: Benchmarking retrieval methods and sensor characteristics for proximal sensing. *Remote Sens.* **11**, 962 (2019).

~~142. Bilger, W. & Björkman, O. Role of the xanthophyll cycle in photoprotection elucidated by measurements of light-induced absorbance changes, fluorescence and photosynthesis in leaves of Hedera canariensis. *Photosynth. Res.* **25**, 173-185 (1990).~~

143. Vilfan, N. *et al*. Extending Fluspect to simulate xanthophyll driven leaf reflectance dynamics. *Remote Sens. Environ.* **211**, 345-356 (2018).

144. Yang, P., Prikaziuk, E., Verhoef, W. & van der Tol, C. SCOPE 2.0: A model to simulate vegetated land surface fluxes and satellite signals. *Geosci. Model Dev. Discuss.*, 1-26 (2020).

145. Gastellu-Etchegorry, J. *et al*. DART: recent advances in remote sensing data modeling with atmosphere, polarization, and chlorophyll fluorescence. IEEE J. Sel. Top. Appl. Earth Obs. Remote Sens. **10**, 2640-2649 (2017).

Corresponding Author: Albert Porcar-Castell, joan.porcar@helsinki.fi

Acknowledgements: This perspective idea originated during the Fluorescence Across Space and Time (FAST) Workshop, which took place in Hyytiälä Forestry Research Station (SMEARII, Finland) during February 2019. We thank the following participants for active discussions during the workshop: Juliane Bendig, Kukka-Maaria Erkkilä, Noda Hibiki, Laura V. Junker-Frohn, Valentyna Kuznetsova, Hannakaisa Lindqvist, Paul Näthe, Jaakko Oivukkamaki, Neus Sabater,

742 Twinkle Solanki, Tea Thum, Shan Xu and Chao Zhang. We also thank Barry Osmond and Josep
743 Peñuelas for valuable comments to the manuscript, to Nuria Altimir for improving graphic design
744 of Figs 1 and 5, and to Bastian Siegmann for the preparation of the HyPlant image in Fig. 3. The
745 Academy of Finland (Project # 288039 and 319211) is acknowledged for the financial support. ZM
746 was supported by the Australian Research Council (FT160100477), TM was supported by the
747 National Aeronautics and Space Administration (80NSSC19M0129), and SVW was supported by
748 the Generalitat Valenciana and the European Social Fund (APOSTD/2018/162). Headwall SIF
749 images from LPA and JRK were supported by grants from the Institute at Brown for Environment
750 and Society at Brown University.

751 **Author contributions:** APC conceived the original idea and wrote the manuscript with ZM, TM,
752 BL, SVW, BFM, FM, YZ, KM with comments and contributions from all co-authors. In addition,
753 these authors had special contribution to the following parts: Fig.1 (APC, ZM and SVW), Fig.2
754 (APC, BFM, TM and SVW), Fig. 3 (LPA, UR and JRK), Fig. 4. (APC, ZM, UR, BFM), Fig. 5
755 (JIGP, JA, ZM, IE), Box 1 (TM, APC), Box 2 (ZM, APC), Supplementary information (ZM, FZ).

756

757

758

759

760

761

762

Figures

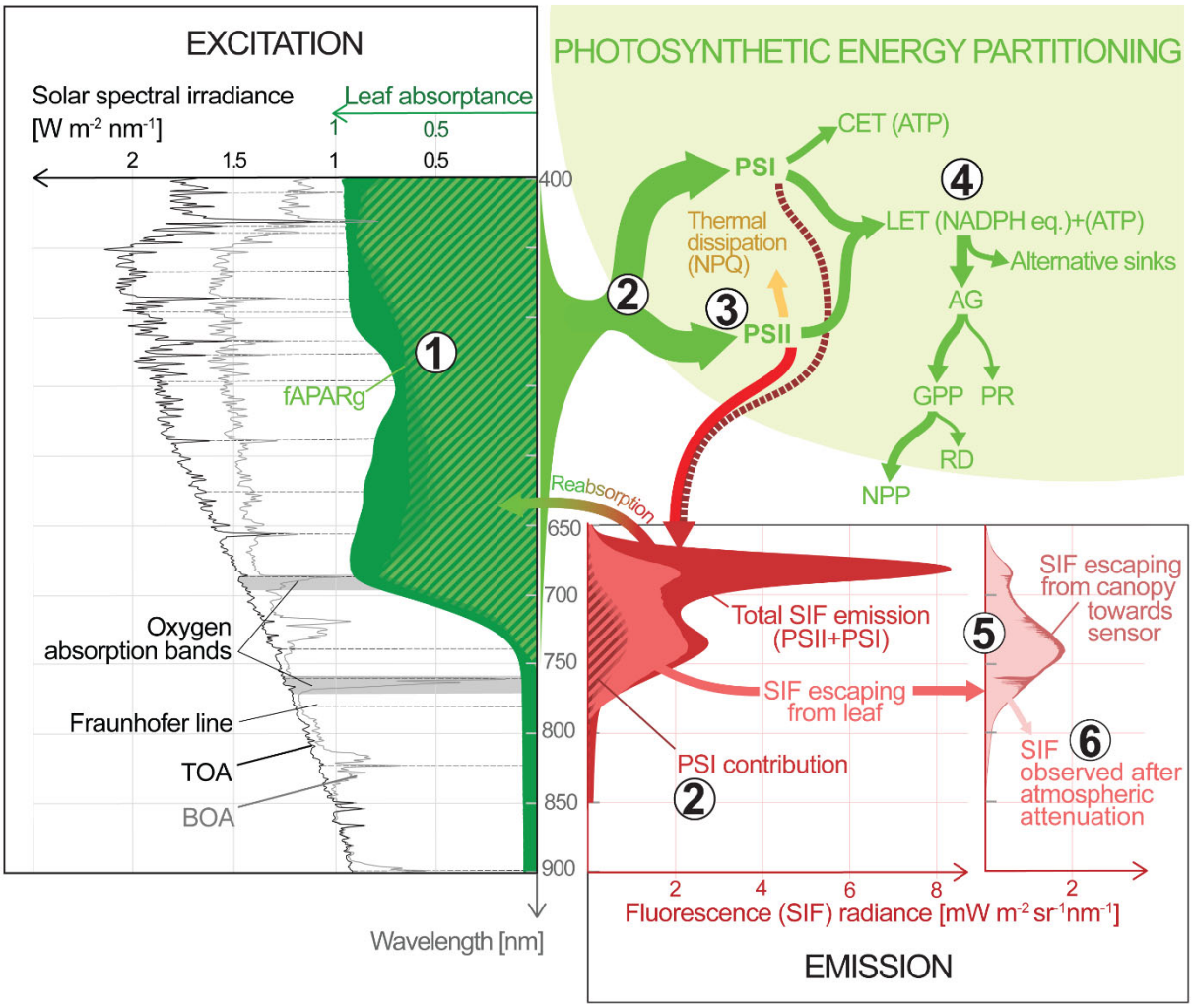

Figure 1. From incoming radiation to observed SIF and photosynthesis: mechanistic challenges. Solar radiation reaching the top of the atmosphere (TOA) is partly absorbed and scattered by atmospheric gases and particles, decreasing its intensity as it reaches the bottom of the atmosphere (BOA) and generating specific absorption features. Part of the radiation is absorbed by photosynthetic pigments in vegetation and leaves ($fAPAR_g$) (**Challenge 1**), associated with either photosystem I (PSI) or photosystem II (PSII), which contribute with differential dynamics and spectral properties to overall SIF emission (**Challenge 2**). Within each photosystem, energy is

773 further partitioned into three dynamic processes (**Challenge 3)**: i) photochemistry (leading mainly
774 to linear (LET) or cyclic (CET) electron transport, the latter involving PSI only), ii) thermal energy
775 dissipation, and iii) ChlaF. Photosynthetic energy (expressed for simplicity in terms of NADPH
776 equivalents) is further partitioned between alternative energy sinks and gross photosynthesis (A_G),
777 and again between gross primary productivity (GPP) and photorespiration (P_R), with dynamics that
778 are not necessarily seen by SIF (**Challenge 4**). Notably, because photosynthetic gas exchange
779 measurements are only able to estimate net flux of CO_2 from a leaf or ecosystem, i.e. net
780 photosynthesis or net primary productivity (NPP), the rate of daytime respiration (R_D) must be
781 known or estimated. In turn, because emitted ChlaF overlaps with the absorption spectra of leaves
782 and plant canopies, some SIF photons - especially those in the red wavelengths - are re-absorbed
783 within the canopy (**Challenge 5)**. Emitted ChlaF is further scattered and absorbed by aerosols and
784 gases in the atmosphere (**Challenge 6**).

785

786

787

788

789

790

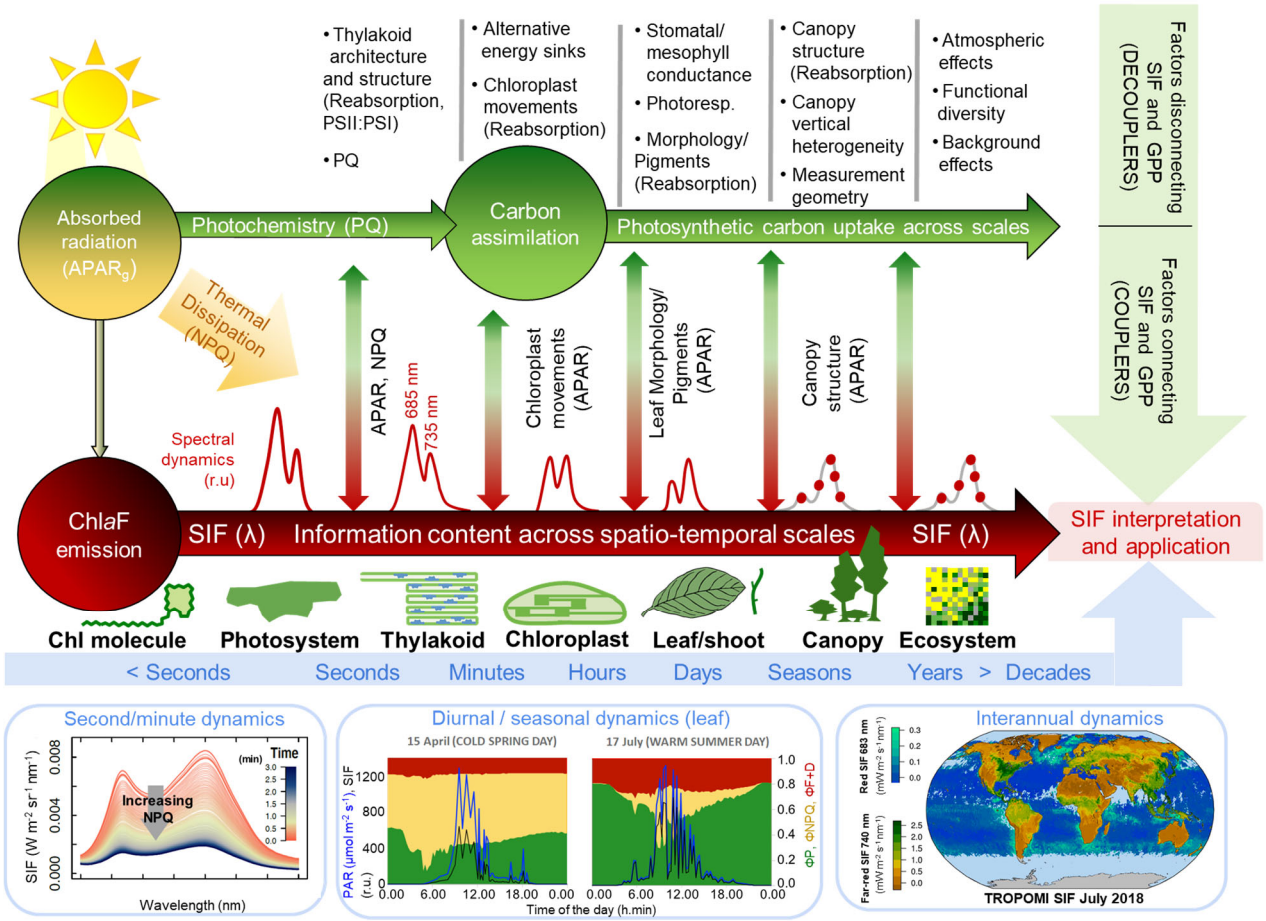

Figure 2. The connection between SIF and GPP across space and time. The relationship between SIF and GPP is affected by multiple factors as we move across spatial and temporal scales. Some factors exert a similar effect on SIF and GPP, keeping them positively correlated - we call these couplers. Other factors differentially affect SIF and GPP - we call these decouplers. Factors driving the dynamics of NPQ and APAR will tend to keep SIF and GPP coupled both across space and time, whereas factors adding variation to the energy partitioning between ChlF and GPP, or influencing the reabsorption of ChlF, will tend to decouple SIF from GPP (see examples in the figure). Note how the shape of the ChlF spectrum ("**Spectral dynamics**") changes across scales in response to reabsorption within the chloroplast, leaf and canopy, measurable as SIF only within discrete wavelengths at the canopy and ecosystem levels (Box 1). Equally important to our understanding of the spatial context of the factors that couple/decouple SIF to GPP is understanding

804 their temporal range of action (lower panels). For example, the rapid (**second/minute**) decrease in
805 ChlaF upon saturating illumination of dark acclimated leaves reflects the dynamics of NPQ[92].
806 Similar dynamics can be seen under natural conditions at the **diurnal/seasona**l scale in Scots pine
807 needles, as the quantum yield of fluorescence (ΦF) responds to PQ and NPQ (redrawn from Porcar-
808 Castell[51]). Here, SIF was estimated for illustrative purposes as SIF (r.u.) = PAR x 0.8 x 0.5 x ΦF,
809 where 0.8 and 0.5 are estimates for $fAPAR_g$ and the fraction of radiation absorbed by PSII.
810 Likewise, **interannual** dynamics at the regional-to-local scales[35] can reflect changes in canopy
811 structure, physiological stress responses or other functional traits. The challenge remains as to how
812 to integrate and disentangle the impact of these couplers/decouplers across space, time, species and
813 plant stress responses (**Challenge 7**).

814

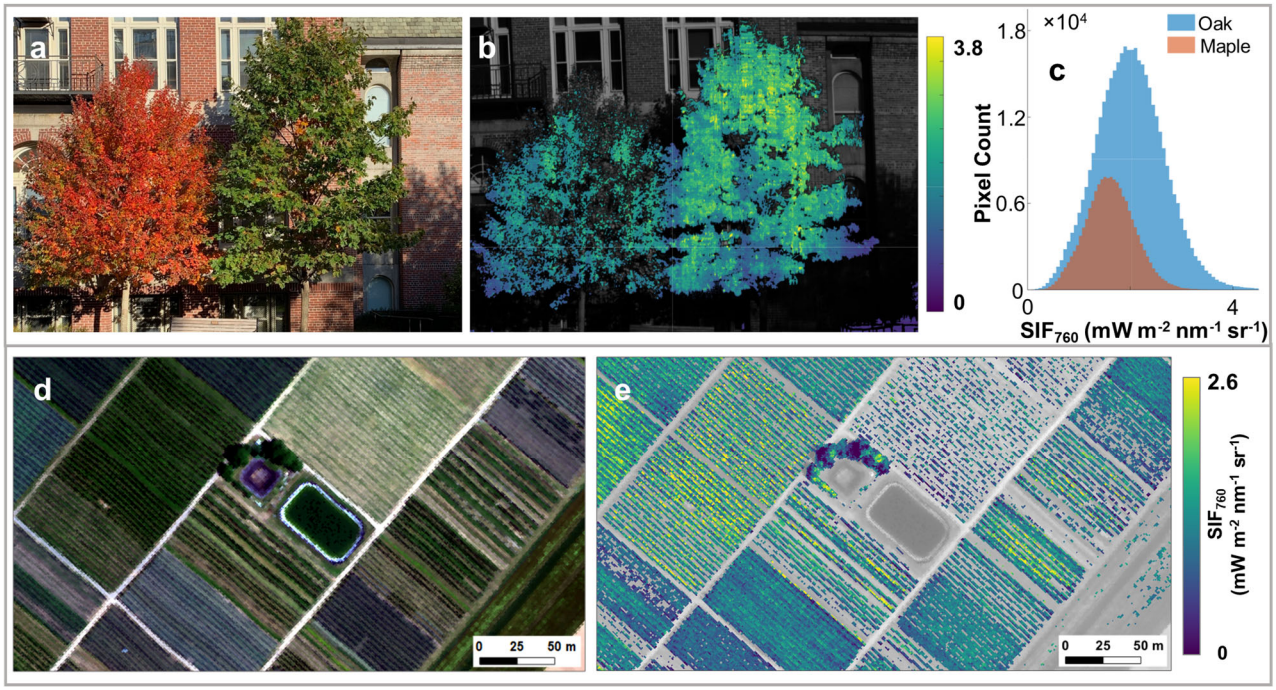

815

816

817 **Figure 3.** State-of-the-art SIF imaging methods allow for the observation of SIF across a continuum
818 of scales: from the leaf-to-individual (top row) to the individual-to-landscape (bottom row). Panel A

819 shows an RGB image of a senescing maple tree next to an oak tree with green leaves. Panel B
820 shows the SIF image of the same trees retrieved in the O2A band at 760 nm (SIF760) using a
821 commercial, off-the-shelf imaging spectrometer[139] mounted on a tripod some meters away and after
822 applying a filter to exclude non-vegetation pixels (pixels with an normalized difference vegetation
823 index (NDVI) < 0.65). As expected, the green and photosynthetically active oak emitted SIF at
824 higher magnitude (Panel C) than the senescing maple. Similarly, panels D-E present an airborne
825 RGB and SIF760 map obtained with data from the HyPlant sensor collected at an altitude of 680 m
826 above ground[111]. The scene shows several plots within an experimental apple tree plantation at the
827 agricultural research site Campus Klein-Altendorf (University of Bonn, Germany), where apple tree
828 varieties of different ages were growing in a typical row structure. Single tree crowns were
829 segmented by overlaying the SIF images with a 3D surface map and all pixels that were related to a
830 background signal (defined as ground level + 30 cm) were excluded. The image visualizes the
831 signal of individual trees, where each pixel corresponds to an area of 1x1 meters and thus the small
832 clusters represent the signal of an individual tree.

833
834
835
836
837
838
839
840
841
842
843

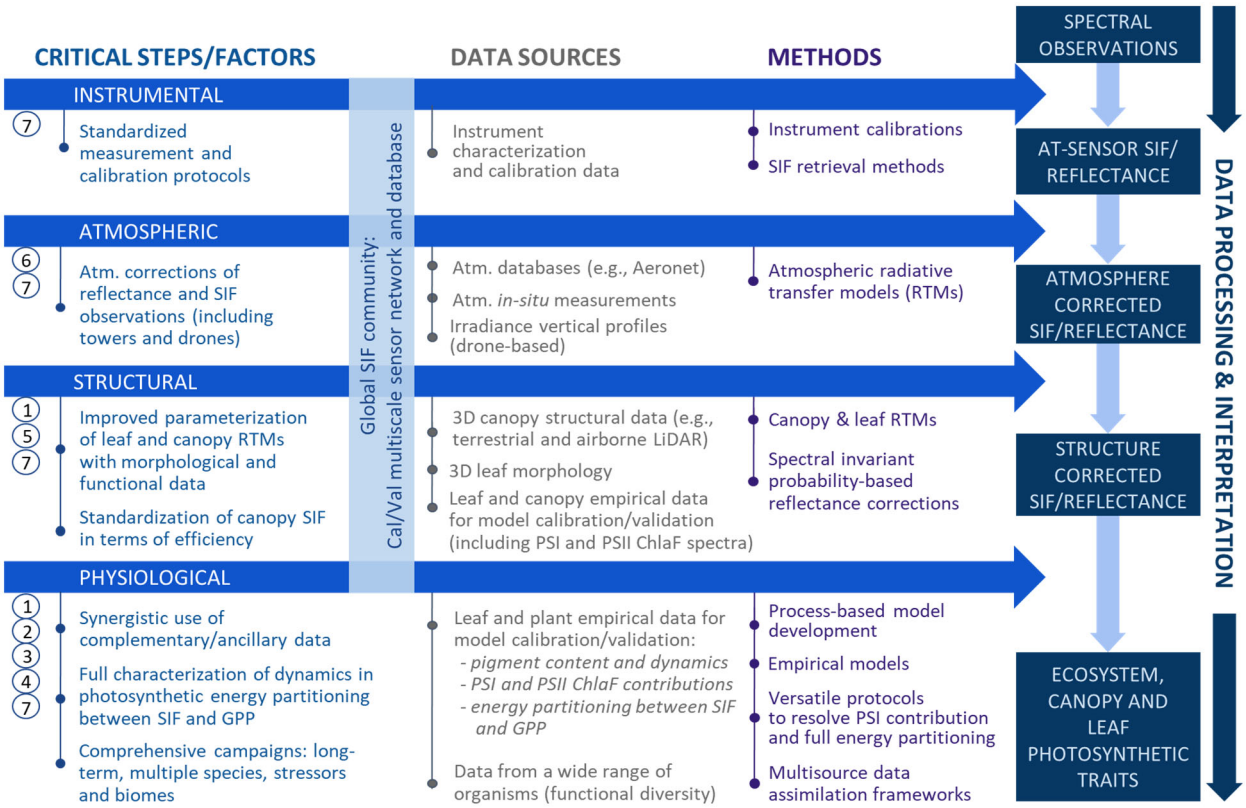

Figure 4. A roadmap towards the standardized interpretation of SIF. The critical steps, data sources and methods that will be required to overcome the seven challenges are introduced to allow for a consistent interpretation of spectral observations in terms of leaf, canopy and ecosystem traits.

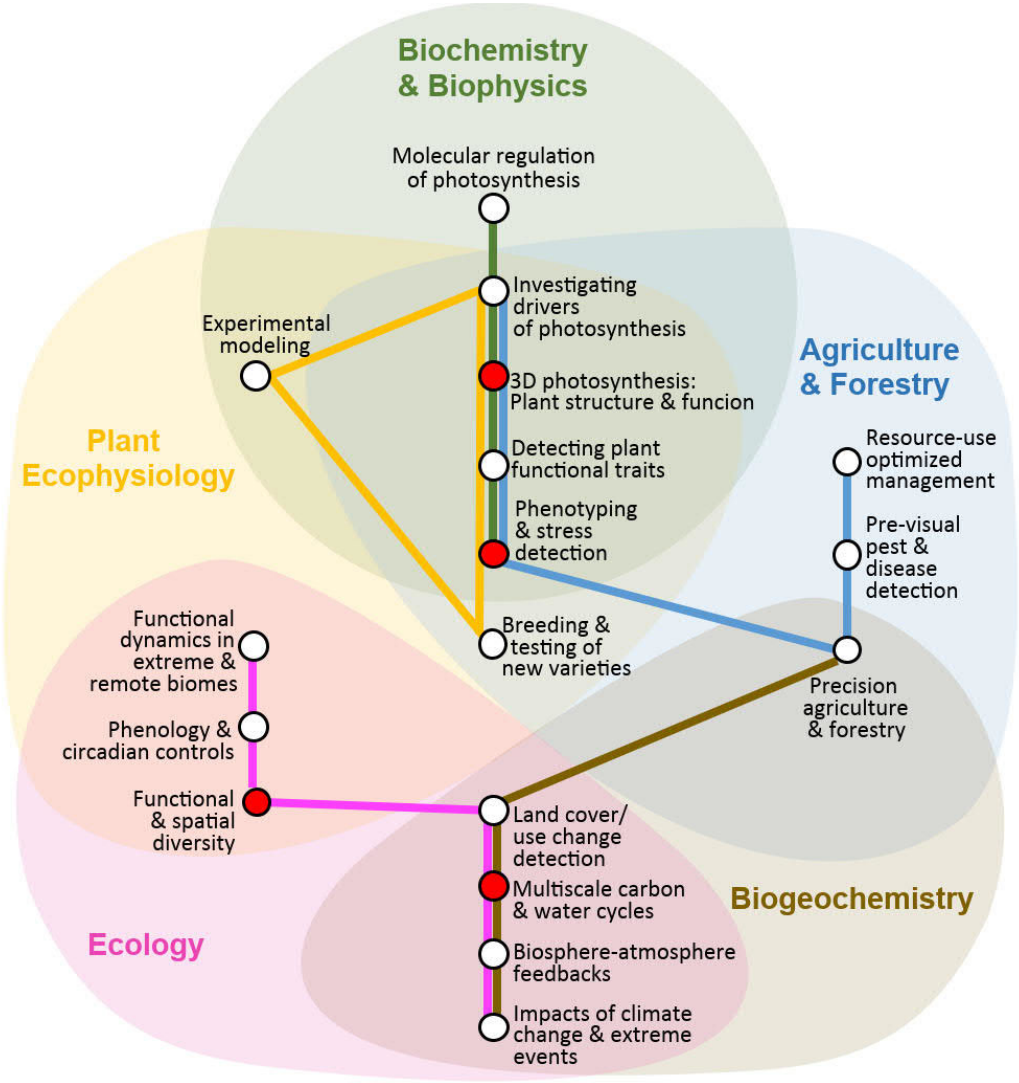

Figure 5. Potential and emerging SIF applications illustrated in the form of a "SIF-city" metro plan, where different colors denote five fields of plant science. Identified research applications (metro stops) are causally connected in individual communication lines, but the final trajectories and number of stops will depend on how the field of SIF research evolves over the next years. The red-colored stops denote the application topics elaborated in Section 3.

Boxes

Box 1 | Principle of solar-induced fluorescence (SIF) retrieval

SIF measurements take place outdoors, under ambient sunlight. Accordingly, when pointing a spectroradiometer towards a leaf or plant canopy to make a SIF measurement, we face the challenge that vegetation is highly reflective in the near infrared (NIR) wavelengths, and the signal is dominated by reflected light. The retrieval of SIF from the background reflected radiation is made possible thanks to the spectral properties of incoming light.

The solar spectrum, as measured above a plant canopy, is not continuous; rather, radiation is strongly attenuated within so-called Fraunhofer absorption lines and telluric absorption bands originating from absorption by gases in the Sun's photosphere or the Earth's atmosphere, respectively (see Fig. 1 and an idealized spectral feature in **A**). These features are exploited by the Fraunhofer line depth (FLD) methods[140] where at least four spectral measurements, usually more[141], are required: the irradiance of the incoming sunlight and the apparent reflected radiance (called apparent, as it includes also SIF), inside and outside of the spectral absorption feature (E_{in}/E_{out} and L_{in}/L_{out}, respectively). Since SIF contributes photons similarly both inside and outside the spectral feature (**B**), the relative contribution of SIF to reflected radiation is significantly greater inside the spectral feature, causing an increase in the apparent reflectance (**C**). This increase is proportional to the amount of SIF and can be used to construct a system of equations to retrieve SIF.

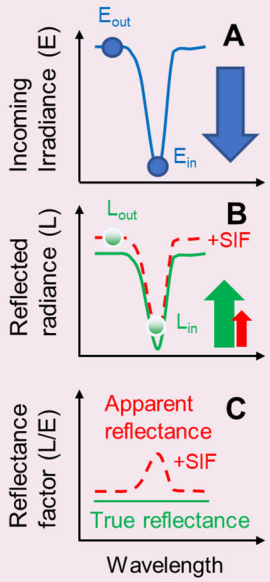

Although not mutually exclusive, SIF measurements are often conducted using either the Fraunhofer or Telluric absorption bands, which involve some trade-offs:

- **Fraunhofer lines** (multiple lines across the SIF spectrum). The advantage of these retrievals lies in their lower sensitivity to atmospheric properties, which is practical for remote measurements as well as applications with variable target-to-sensor distances (e.g., multiangular tower measurements). The main disadvantage is that they require spectrometers with extremely high spectral resolutions and generally require longer periods of signal integration.
- **Telluric bands** (mainly oxygen absorption bands B and A, centered around 687-692 nm; and 759-770 nm, respectively). Since these bands are broader, measurements do not require as high spectral resolution and can be also conducted with shorter integration time, which can be especially suitable for some applications (e.g. drone-based observations). Their main disadvantage is that attention must be paid to corrections for atmospheric absorption (Challenge 6).

880

881

Box 3 | Radiative transfer models (RTMs)

- **Forward mode.** When the required inputs are provided, RTMs are capable of simulating leaf and canopy SIF together with reflected and emitted optical and thermal radiance. Once successfully validated by independent measurements, RTMs can be used in the forward mode to investigate the sensitivity of outputs, (i.e., surface reflectance and SIF) to different structural, biochemical, and physiological inputs, extending our mechanistic understanding of reflected and emitted photons' propagation across scales.
- **Inverse mode.** RTMs can be also inverted (i.e., run backwards) to estimate from laboratory, field and remote sensing spectral data those leaf and canopy traits that match measured reflectance and SIF data.

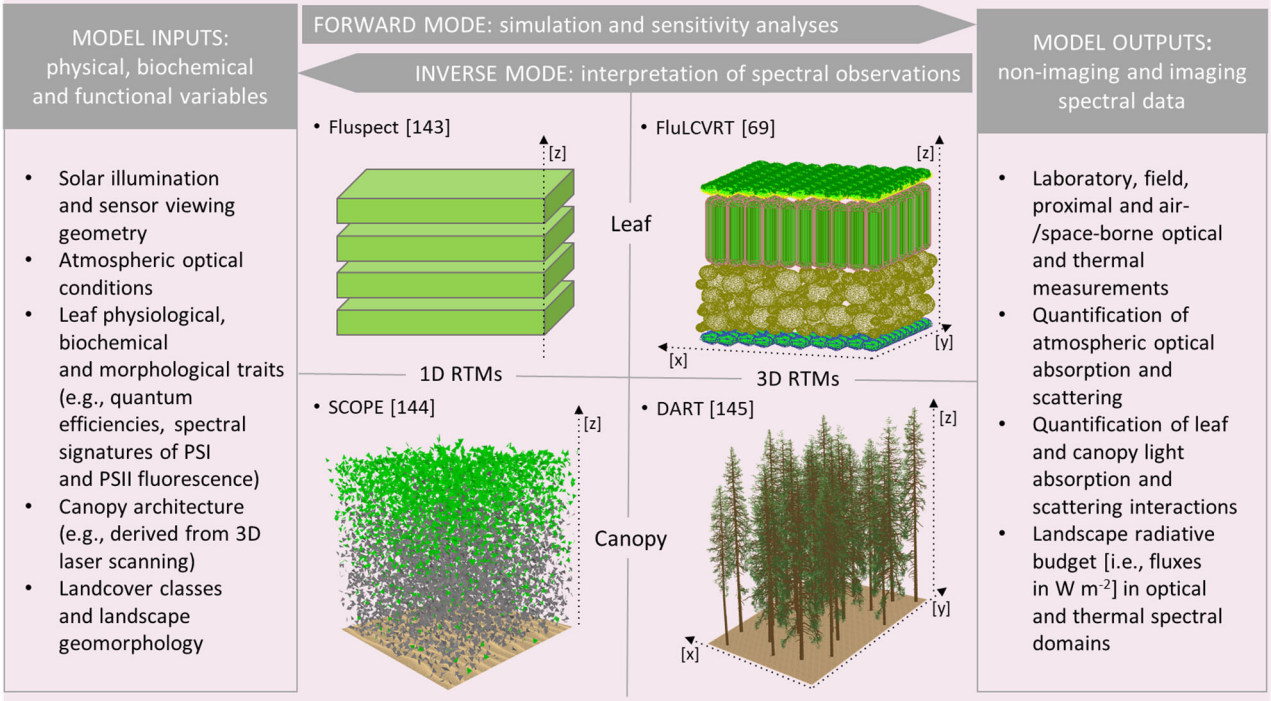

- **1D models.** 1D leaf RTMs assume that leaf constituents are horizontally homogeneously distributed in vertically stacked plate structures, and hence require only basic morphological and biochemical inputs (e.g., pigment contents driving PAR absorption and within-leaf reabsorption, the intrinsic PSII and PSI fluorescence spectra, and the dynamics in the quantum yield of fluorescence as the mechanistic link to photosynthesis). This simplicity, however, ignores potentially important factors, such as within-leaf heterogeneity or chloroplast movements. As with the 1D leaf construct, 1D canopy RTMs assume that vegetation can be represented by horizontally homogeneous layers filled with leaves of a predefined size, density and geometry (angular distribution), which allows for minimal model inputs and a relatively straightforward application. The 1D architecture has its uses for spatially homogeneous canopies (e.g., crops).
- **3D models.** Structurally complex leaves and spatially heterogeneous plant communities (e.g., forests and savannas) require 3D representations. 3D leaf RTMs can model optical interactions within a genuine 3D digital representation of leaf interior reconstructed, for example, with imaging tomography or confocal microscopy. As demonstrated in the Supplementary Videos 1 and 2, 3D RTM solutions also exist for spatially diversified plant canopies, allowing for accurate physical simulations of $APAR_g$ and SIF fluxes in complex canopies.

882